

# DEVELOPMENT OF AN APF IH-DTL IN THE J-PARC MUON $g - 2$ /EDM EXPERIMENT

Y. Nakazawa\*, H. Iinuma, Ibaraki University, Mito, Ibaraki, Japan  
Y. Iwata, National Institute of Radiological Sciences, Chiba, Japan  
M. Otani, N. Kawamura, T. Mibe, E. Cicek, T. Yamazaki, M Yoshida  
KEK, Tsukuba, Ibaraki, Japan

R. Kitamura, Y. Kondo, T. Morishita, JAEA, Tokai, Naka, Ibaraki, Japan  
N. Saito, J-PARC center, Tokai, Naka, Ibaraki, Japan  
Y. Sue, K. Sumi, M. Yotsuzuka, Nagoya University, Nagoya, Japan  
Y. Takeuchi, Kyushu University, Fukuoka, Japan  
N. Hayashizaki, Tokyo Institute of Technology, Tokyo, Japan  
H. Yasuda, University of Tokyo, Hongo, Tokyo, Japan

## Abstract

An inter-digital H-mode drift-tube linac (IH-DTL) is under development in a muon linac at the J-PARC muon  $g - 2$ /EDM experiment. It accelerates muons from 0.34 MeV to 4.3 MeV at an operating frequency of 324 MHz. The cavity can be miniaturized by introducing the alternative phase focusing (APF) method that enables transverse focusing only with an E-field. A three-dimensional field analysis modeled the APF IH-DTL cavity, and the beam dynamics were evaluated numerically. The beam emittance was calculated as  $0.316 \pi$  and  $0.189 \pi$  mm mrad in the horizontal and vertical directions. The field error due to the fabrication errors and thermal expansion during operation causes an emittance growth. We evaluated that the optimized tuners can suppress the emittance growth to less than 10%. In this paper, the detailed design of the APF IH-DTL, including the tuner, will be reported.

## INTRODUCTION

The anomalous magnetic moment of muons (muon  $g - 2$ ) is significant for physics beyond the standard model (SM). The Fermi National Accelerator Laboratory (FNAL-E989) measured the muon  $g - 2$  with an accuracy of 0.46 ppm [1] and showed a discrepancy of 4.2 standard deviations from the SM prediction [2], consistent with the previous experiment BNL-E821 [3]. We plan the J-PARC muon  $g - 2$ /EDM experiment (E34) [4] as a precision measurement with a completely independent approach from the previous experiment to ensure the validity of this discrepancy. The E34 experiment aims to measure the muon  $g - 2$  of 0.1 ppm accuracy. In order to suppress beam-derived systematic errors, low-emittance muon beams are required, and the development of an original muon linear accelerator (linac) is essential. Muons are accelerated from thermal energy to relativistic energy using four RF linacs depending on the beam velocity [5].

We adopted an IH-DTL [6] with high acceleration efficiency in the low-speed region at a second stage to suppress

the muon decay loss during acceleration. Moreover, an alternative phase focusing (APF) method, which enables transverse focusing using only an RF electric field, is introduced to realize a compact cavity. On the other hand, since the APF method uses the RF field for beam focusing, the field error of the on-axis electric field significantly affects the beam dynamics. When the experimental tolerance of emittance growth is approximately 10% or less, we should suppress the field error from the design value to less than  $\pm 2\%$  [7]. A required field distribution is usually reached after several tuning iterations by hand. On the other hand, in our approach, the optimal solution of the tuning is mathematically derived by using the singular value decomposition (SVD) [8] of the matrix created by CST MICROWAVE STUDIO (MWS) [9].

This paper proceeds as follows. After introducing the basic design of the IH-DTL, we quantitatively estimated the field error. Then, we present that the tuning algorithm using SVD can be applied to correct the field error. Finally, we summarize the results and discuss prospects.

## APF IH-DTL DESIGN

The cavity and dynamics of the IH-DTL were designed based on the basic model [6]. Figure 1 shows the three-dimensional electromagnetic field analysis model of the IH-DTL, and Table 1 shows the basic parameters.

The cavity consists of 16 cells and excites the  $TE_{111}$  mode as the operation mode. We plan to assemble the cavity in a three-piece structure made of oxygen-free copper, consisting of a center plate with a drift tube and two side plates.

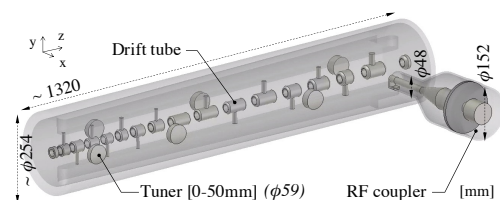


Figure 1: APF IH-DTL 3D-model in CST MWS.

\* 20nd103s@vc.ibaraki.ac.jp

Table 1: Basic Parameters of the APF IH-DTL

Operation frequency	324 (MHz)
$Q_0$	$1.04 \times 10^4$
Maximum E	$1.98 E_k$ (MV/m)
Nominal peak power	322 (kW)
Duty	0.1 %
Injection energy	0.34 (MeV)
Extraction energy	4.26 (MeV)
$\varepsilon_{x, \text{rms}, n}$	0.316 ( $\pi$ mm mrad)
$\varepsilon_{y, \text{rms}, n}$	0.189 ( $\pi$ mm mrad)

The tuners and RF couplers were newly designed based on the experience in the IH-DTL prototype of the six-cell model [10, 11] developed for the performance test. The six tuners are  $\varnothing 59$  mm in diameter, with a range of insertion length of 0–50 mm, and we equally spaced these for the number of cells. The RF coupler utilizes alumina ceramics for the RF window, and an impedance matching to the cavity is adjusted by rotating the magnetic loop.

## ERROR FIELD STUDY

The causes of the field error in the on-axis field are considered field variations due to structural displacement of the cavity caused by fabrication errors and thermal expansion. We quantitatively estimated the effect of each of these factors on the on-axis electric field as follows.

First, we estimated the fabrication error by measuring the fabricated prototype IH-DTL. The fabrication errors of the drift tube radius and the distance between cells were measured to be fewer than  $50 \mu\text{m}$  and  $190 \mu\text{m}$ , respectively, using a three-dimensional measuring instrument. The same fabrication errors are expected for the real IH-DTL.

Next, we estimated the thermal expansion of the cavity during high power operation by CST MPHYSICS STUDIO (MPS). A detailed engineering structure was simulated, including six water cooling channels designed to suppress heat and stabilize the frequency. Figure 2(a) shows the results of steady thermal analysis in the cavity with cooling channels. The heat transfer coefficient of the cavity surface was  $14 \text{ W/m}^2 \cdot \text{K}$ , assuming natural convection. Moreover, the water pipe was  $6980 \text{ W/m}^2 \cdot \text{K}$  calculated from the pipe diameter and water velocity. The maximum temperature rise in the drift tube with the highest surface current density is about 9 degrees. And then, we simulated the displacement due to the stress, as shown in Fig. 2(b). The maximum position displacement of the drift tube in the  $z$ -direction was  $60 \mu\text{m}$ . Based on these estimations, the local structural displacement of fewer than 100–200  $\mu\text{m}$  is expected.

We intentionally changed some dimensions of the cavity model in CST MWS to estimate the variation of the electric field depending on the structural displacement. Figure 3 shows the on-axis field variation when the 1<sup>st</sup> drift tube is displaced in the position in the  $z$ -axis.

MC4: Hadron Accelerators

A09 Muon Accelerators and Neutrino Factories

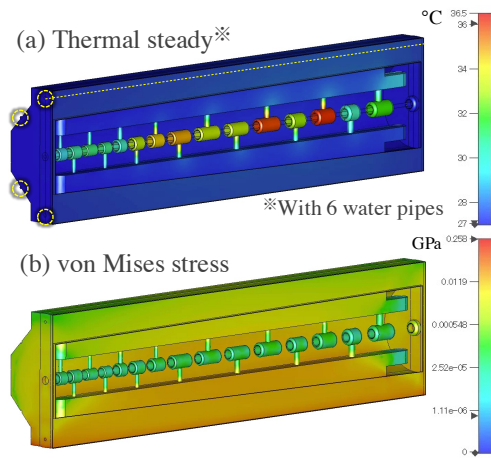


Figure 2: (a) The result of the steady thermal simulation of the engineering structure with six water channels. The ambient temperature and the initial temperature of the water are 27 degrees. (b) The result of the von Mises stress of the mechanics' simulation.

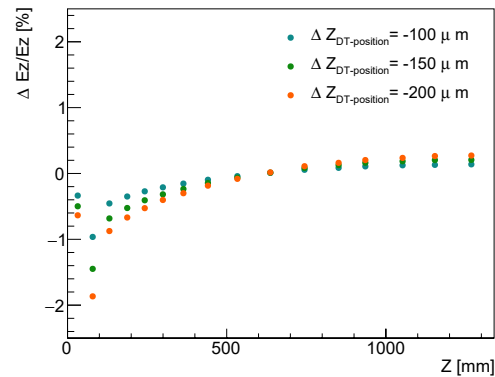


Figure 3: The on-axis field variation in each cell gap when the 1<sup>st</sup> drift tube is displaced in the  $z$ -direction.

Other dependence such as the drift tube radius, vertical positions, and the slant were also simulated. After examining all the results, we found that the local structural displacements of fewer than  $200 \mu\text{m}$  cause field errors of less than  $\pm 2\%$ .

## TUNING

If the field error due to the local structural displacement of  $200 \mu\text{m}$  occurs at several drift tubes, it will exceed the allowable emittance growth of 10%. Therefore, we use an insertion tuner to correct the field error of less than  $\pm 2\%$ . It is also required to tune the cavity to the resonant frequency ( $324 \pm 0.01$  MHz) within the operating range of the tuner insertion.

The tuning algorithm is based on a response matrix describing the effect of six tuners on the field distribution at 16 cells. Figure 4 shows the variation of the on-axis electric field in each cell gap for a single tuner.

WEXB06

2545

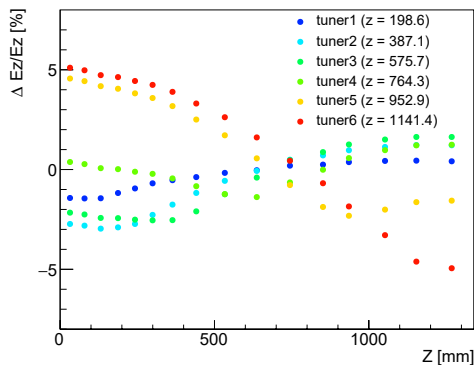


Figure 4: The on-axis field variation in each cell gap when only a single tuner is placed in six positions in the  $z$ -direction.

The field variation due to the tuner depends on the distribution of the second higher-order mode  $TE_{112}$ , which resonant frequency is about 6 MHz higher than the operation mode  $TE_{111}$ . Furthermore, since the field variation for the tuner insertion proved good linearity, the response matrix becomes

$$\Delta E_i = \sum_j \frac{\partial E_i}{\partial L_j} L_j, \quad (\vec{\Delta E} = \mathbf{M} \cdot \vec{L}). \quad (1)$$

Where  $E_i$  is the on-axis electric field of the  $i$ th gap,  $L_j$  is the insertion volume of the  $j$ th tuner, and  $\partial E_i / \partial L_j$  is the response matrix of the  $j$ th tuner, which will be referred to as  $\mathbf{M}$ . The initial tuner insertion is 0 mm with a flush position. The response matrix for the resonant frequency was also created in the same way.

Since the response matrix of the field is non-regular, we use SVD to solve this inverse problem. SVD allows us to arbitrarily truncate higher-order eigenmodes to use in the optimization calculation, unlike the least-squares. Thus, it enables us to make field corrections that satisfy our requirements while selecting feasible solutions for resonant frequency and tuner settings. In this case, the field tuning algorithm follows

$$\vec{L} = \mathbf{M}^+ \cdot \vec{\Delta E}, \quad (\mathbf{M}^+ = \mathbf{V}^{-1} \mathbf{U}^T). \quad (2)$$

Where  $\mathbf{U}$  is the orthogonal matrix ( $16 \times 16$ ) of the field variation,  $\mathbf{V}$  is also the orthogonal matrix ( $6 \times 6$ ) of the tuner condition, and is the diagonal matrix with the singular values of the response matrix  $\mathbf{M}$  as the diagonal elements.

Finally, a case study assuming a local structural displacement of fewer than  $200 \mu\text{m}$  was performed. We selected the truncation eigenmode number to obtain the optimal solution using the tuning algorithm and then simulated it again in CST MWS using the tuning settings obtained from our calculations. There are two possible truncation methods: Tikhonov's regularization and the truncated SVD method, yielding similar results. For example, Fig. 5 shows the corrected field error using Tikhonov's regularization.

This algorithm corrects the peak-to-peak of the field error to 2.5% within the tuner insertion range, and the resonant

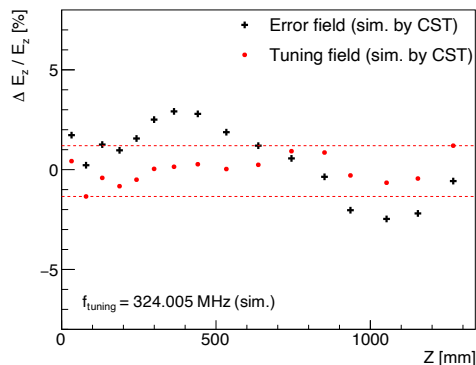


Figure 5: Case study result of the field and frequency tuning. (Black) The simulated field error due to the structural displacement of fewer than  $200 \mu\text{m}$ . (Red) corrected field by Tikhonov's regularization method.

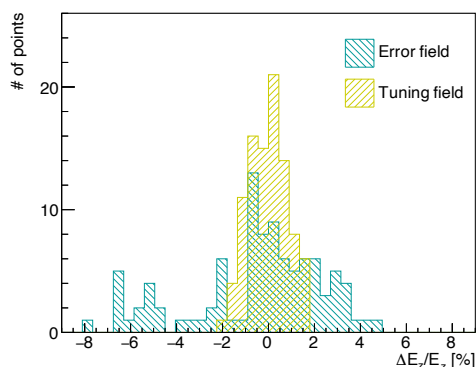


Figure 6: Field error on each gap in a summary of 6 times case study. The structural displacements of  $200\text{-}300 \mu\text{m}$  were assumed.

frequency also satisfied the requirement. In addition, the different case study was performed six times, as shown in Fig. 6. We confirmed that the six tuners were able to correct the field error from the design value within the required value of less than  $\pm 2\%$ .

## SUMMARY AND PROSPECT

We are currently developing the APF IH-DTL for the muon  $g - 2$ /EDM experiment. The field error of about 2% due to structural displacement can be corrected to satisfy the experimental requirements of dynamics by applying the tuner algorithm using SVD. The detailed engineering design, including cooling channels, tuners, and RF coupler, has already been completed, and we plan to fabricate it.

## ACKNOWLEDGEMENTS

This work is supported by JSPS KAKENHI Grant Numbers JP15H03666, JP18H03707, JP16H03987, JP16J07784, and JP20J21440.

## REFERENCES

- [1] B. Abi *et al.*, “Measurement of the Positive Muon Anomalous Magnetic Moment to 0.46 ppm”, *Phy. Rev. Lett.*, vol. 126, no. 14, p. 141801, Apr. 2021. doi:10.1103/PhysRevLett.126.141801
- [2] T. Aoyama *et al.*, “The anomalous magnetic moment of the muon in the Standard Model”, *Physics Reports*, vol. 887, pp. 1–166, 2020. doi:10.1016/j.physrep.2020.07.006
- [3] G. W. Bennett *et al.*, “Final report of the E821 muon anomalous magnetic moment measurement at BNL”, *Phy. Rev. D*, vol. 73, no. 7, p. 072003, Apr. 2006. doi:10.1103/PhysRevD.73.072003
- [4] M. Abe *et al.*, “A New Approach for Measuring the Muon Anomalous Magnetic Moment and Electric Dipole Moment”, *Prog. Theor. Exp. Phys.*, vol. 2019, no. 5, May 2019. doi:10.1093/ptep/ptz030
- [5] Y. Kondo *et al.*, “Re-Acceleration of Ultra Cold Muon in JPARC Muon Facility”, in *Proc. IPAC’18*, Vancouver, BC, Canada, Apr.-May 2018, pp. 5041–5046. doi:10.18429/JACoW-IPAC2018-FRXGBF1
- [6] M. Otani *et al.*, “Interdigital H-mode drift-tube linac design with alternative phase focusing for muon linac”, *Phy. Rev. Accel. Beams*, vol. 19, no. 4, p. 040101, Apr. 2016. doi:10.1103/PhysRevAccelBeams.19.040101
- [7] M. Otani *et al.*, “Interdigital H-mode drift-tube linac design with alternative phase focusing for muon linac”, in *Proc. PASJ’16*, Chiba, Japan, Aug. 2016, pp. 858–862, TUP017.
- [8] B. Koubek *et al.*, “rf measurements and tuning of the 750 MHz radio frequency quadrupole”, *Phy. Rev. Accel. Beams*, vol. 20, no. 8, p. 080102, Aug. 2017. doi:10.1103/PhysRevAccelBeams.20.080102
- [9] CST Studio Suite, Computer Simulation Technology (CST), <https://www.cst.com/products/CSTMWS>
- [10] Y. Nakazawa *et al.*, “Prototype of an inter-digital H-mode drift-tube linac for muon linac”, in *Proc. LINAC’18*, Beijing, China, Sep. 2018, pp. 180–183. doi:10.18429/JACoW-LINAC2018-MOP0085
- [11] Y. Nakazawa *et al.*, “Development of inter-digital H-mode drift-tube linac prototype with alternative phase focusing for a Muon Linac in the J-PARC Muon  $g - 2$ /EDM Experiment”, in *Proc. IPAC’19*, Melbourne, Australia, May 2019, pp. 606–609. doi:10.18429/JACoW-IPAC2019-MOPRB017